Heavy absorption and soft X-ray emission lines in the XMM–Newton spectrum of the Type 2 radio-loud quasar 3C 234

E. Piconcelli[1], S. Bianchi[2], G. Miniutti[3], F. Fiore[1], M. Guainazzi[4], E. Jimenez-Bailon[5], G. Matt[2]

[1] Osservatorio Astronomico di Roma (INAF), Via Frascati 33, I–00040 Monteporzio Catone (Roma), Italy
[2] Dipartimento di Fisica, Università degli Studi Roma 3, Via della Vasca Navale 84, I–00146 Roma, Italy
[3] Institute of Astronomy, Madingley Road, Cambridge CB3 0HA, UK
[4] European Space Astronomy Center of ESA, Apartado 50727, E–28080 Madrid, Spain
[5] Instituto de Astronomía, UNAM, Apartado 70264, 04510 Ciudad de México, Mexico

ABSTRACT

Aims. We report results on a 40 ks *XMM–Newton* observation of the Type 2 quasar 3C 234. Optical spectropolarimetric data have demonstrated the presence of a hidden broad-line region in this powerful ($M_V \leq -24.2$ after reddening and starlight correction) narrow-line FRII radio galaxy. Our analysis is aimed at investigating the X-ray spectral properties of this peculiar source which have remained poorly known so far.
Methods. We analyze the 0.5–10 keV spectroscopic data collected by the *EPIC* cameras in 2006.
Results. The X-ray spectrum of this radio-loud quasar is typical of a local Compton-thin Seyfert 2 galaxy. It exhibits strong absorption ($N_H \sim 3.5 \times 10^{23}$ cm^{-2}) and a narrow, neutral Fe Kα emission line with an equivalent width of $\approx 140\pm40$ eV. Our observation also reveals that the soft portion of the spectrum is characterized by strong emission lines with a very low level of scattered primary continuum. A possible explanation of these features in terms of thermal emission from a two-temperature collisionally ionized plasma emission seems to be unlikely due to the high luminosity estimated for this component ($L_{0.5-2} \sim 6 \times 10^{42}$ erg s^{-1}). It is likely that most of the soft X-ray emission originates from a photoionized plasma as commonly observed in obscured, radio-quiet Seyfert-like AGNs.
Conclusions. This X-ray observation has definitively confirmed the presence of a hidden quasar in 3C 234. The line-rich spectrum and the steepness of the hard X-ray continuum ($\Gamma \approx 1.7$) found in this source weaken the hypothesis that the bulk of the X-ray emission in radio-loud AGNs with high excitation optical lines arises from jet non-thermal emission.

Key words. Galaxies: active – Galaxies: nuclei – Quasars: individual: 3C 234 – X-ray: galaxies

1. Introduction

Type 2 quasars (QSO2s hereafter) are usually defined as those active galactic nuclei with the following properties: (i) a highly (i.e. $N_H \geq 10^{22}$ cm^{-2}) absorbed X-ray emission (ii) an intrinsic, hard X-ray (i.e. 2-10 keV) luminosity $\geq 10^{44}$ erg s^{-1}, and (iii) the lack of broad emission lines in their optical/UV spectra (the latter condition is often overcome since these objects are usually too weak, i.e. $R \gtrsim 25$ mag, for optical spectroscopy). QSO2 are therefore the luminous counterpart of Seyfert 2 galaxies. Even if their existence was postulated by the AGN unification model (Antonucci 1993; Urry & Padovani 1995) QSO2 have represented for many years the long-sought missing AGN population (Halpern et al. 1999).

Optical and soft X-ray (0.5-2 keV) surveys, being strongly biased by obscuration, fail to detect clearcut examples of such objects. However, over the past ∼10 years, a very limited number of genuine QSO2s have been discovered (e.g. Brandt et al. 1997; Franceschini et al. 2000; Norman et al. 2002; Stern et al. 2002; Della Ceca et al. 2003; Iwasawa et al. 2005; Gandhi et al. 2006) thanks to X-ray observations above 2 keV. In particular, the recent deep and wide-area hard X-ray surveys performed with

Chandra and *XMM–Newton* (e.g. Mainieri et al. 2002; Fiore et al. 2003; Brandt & Hasinger 2005, Eckart et al. 2006; Wang et al. 2007; Georgantopolous et al. 2007; Lacy et al. 2007) have efficiently detected several dozens of QSO2 candidates. Unfortunately, most of them are sources with weak optical emission, showing a very high X-ray–to–optical flux ratio (X/O > 10), and, therefore, with no reliable information about their redshift and classification (e.g. Maiolino et al. 2006). Furthermore, these hard X-ray surveys have established that the obscured AGN fraction decreases with increasing hard X-ray luminosity (Ueda et al. 2003; Steffen et al. 2003; La Franca et al. 2005; Akylas et al. 2006) and strongly increases with the hard X-ray flux only at $F_{2-10} \lesssim 10^{-14}$ erg cm^{-2} s^{-1} (Piconcelli et al. 2003). The combination of these findings explains the difficulties met so far in collecting a large sample of intrinsically-luminous, heavily obscured AGNs. According to the most up-to-date version of the synthesis model of the cosmic X-ray background (CXB), e.g. Gilli, Comastri & Hasinger (2007), the population of obscured QSOs accounts for ∼15% of the CXB in the 2–10 keV band.

Selecting sources with large [OIII] luminosity (i.e. $L_{[OIII]} \gtrsim 10^{42}$ erg s^{-1}) (Derry et al. 2003; Vignali et al. 2006; Ptak et al. 2006) or with AGN luminosities in the mid-infrared and faint optical/near-infrared emission (Martinez-Sansigre et al. 2005; Houck et al. 2005) are the two alternative ap-

proaches which have been proven to be efficient in discovering large samples of QSO2s candidates.

However, given the faintness in the 0.5-10 keV band ($F_{0.5-10} \lesssim 10^{-14}$ erg cm^{-2} s^{-1}) of most of the QSOs candidates detected so far, only for a handful of these objects has been possible to perform meaningful X-ray spectroscopy and, therefore, obtain tight constraints on the absorbing column density and, in general, on their X-ray properties, which are largely unexplored so far (e.g. Akiyama et al. 2002; Severgnini et al. 2006; Piconcelli et al. 2007a).

In this paper, we present a $\sim$40 ks *XMM–Newton* observation of 3C 234, a radio galaxy with Fanaroff-Riley II edge-brightened morphology at $z = 0.1848$ (Riley & Pooley 1975). 3C 234 was initially classified as a broad line radio-galaxy owing to the presence of a weak broad Hα emission line in its optical spectrum (Grandi & Osterbrock 1978). However, Antonucci (1982) and Antonucci (1984) found that both the optical/UV continuum and the broad Hα emission are highly polarized at a position angle perpendicular to the radio axis (with evidence that the broad line is more polarized than the continuum), while the narrow emission lines are very strong (L$_{[OIII]}$ $\sim$1.5 $\times$ 10^{43} erg s^{-1}) and unpolarized. Furthermore, indications of strong extinction can be inferred by the absence of the blue-UV emission bump and the large broad-line Balmer decrement. On the basis of these findings, Antonucci & Barvainis (1990) interpreted the polarization in terms of scattered light from the obscured continuum and broad line region by a population of hot electrons and/or opaque dust clouds (e.g. Kishimoto et al. 2001 for further details) and proposed a narrow line radio galaxy (NLRG) classification for this source. Tran et al. (1995, T95 hereafter) presented the analysis of high signal-to-noise (S/N) Keck spectropolarimetric data for 3C 234 and confirmed that the broad lines are caused by scattered light (Young et al. 1998; Cohen et al. 1999). Applying corrections for reddening and starlight contamination, T95 inferred an absolute magnitude of M$_V \leq -24.2$, i.e. well within the quasar range. All these pieces of evidence indicate that 3C 234 harbors a buried luminous quasar in the nucleus i.e. this source is a Type 2 quasar. Although affected by a low S/N ratio, the *ASCA* spectrum of 3C 234 (Sambruna et al. 1999) provided further support to this classification suggesting the presence of strong absorption (N$_H \sim 10^{23}$ cm^{-2}), an ultra-flat continuum ($\Gamma \sim 0.07$) and a 2-10 keV luminosity of $\sim 10^{44}$ erg s^{-1}.

We adopt a ΛCDM cosmology with H_0=70 km s^{-1} Mpc^{-1} and $\Omega_\Lambda = 0.73$ (Spergel et al. 2007). For 3C 234 at $z = 0.1848$, 1 arcsecond corresponds to a physical scale of 3.1 kpc.

2. XMM–Newton observation and data reduction

3C 234 was observed by *XMM–Newton* (Jansen et al. 2001 and reference therein) on April 24, 2006 for $\sim$40 ks. Data were reduced with SAS 6.5 using standard procedures. X–ray events corresponding to patterns 0–12(0–4) for the *MOS(PN)* cameras were selected. The event lists were filtered to ignore periods of high background flaring according to the method presented in Piconcelli et al. (2004) based on the cumulative distribution function of background light
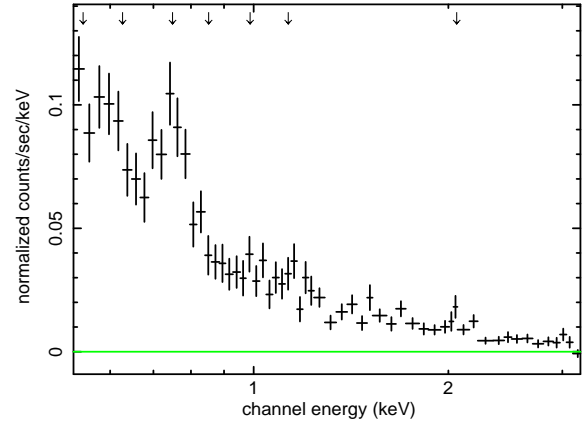

Fig. 1. The soft X-ray portion of the *PN* spectrum of 3C 234 when the hard X-ray *baseline* model (i.e. absorbed power-law continuum + narrow Fe Kα line) is applied to the 0.5–10 keV band. A large soft X-ray excess dominated by several emission line-like features is seen. The arrows indicate the observer-frame energy of the significantly detected emission lines as listed in Table 2.

curve count-rates. After this data cleaning, we obtained a net exposure time of 34.5 ks for the *PN* and of $\sim$38 ks for the two *MOS* cameras. The source spectra were extracted using a circular region of 25 and 32 arcsecs radius for *PN* and *MOS*, respectively, centered on the peak of the X-ray emission at $\alpha_{2000} = 10^h 01^m 49.8^s$ and $\delta_{2000} = +28°47'08''$. The *PN(MOS)* background was estimated from a source–free region with a radius of 66(50) arcsec in the same chip. Response matrices and ancillary response files were generated using the RMFGEN and ARFGEN tools in the SAS. Combined *MOS* spectrum and response matrix were created. Events outside the 0.5-10 keV range were discarded in the *PN* spectrum, while we ignored *MOS* data below the 0.8 keV due to the presence of cross-calibration uncertainties between the *MOS* cameras (Kirsch 2006). Both *PN* and *MOS* spectra were grouped to have a minimum of 20 counts per bin to apply the χ^2 minimization technique, and fitted simultaneously.

During the observation the source flux remained steady, with no variation exceeding 2σ from the average count-rate level in both soft- and hard-X-ray band and no significant spectral changes. Therefore our spectral analysis was performed on the spectrum integrated over the whole good exposure time.

2.1. Spectral analysis

All fits were performed using the XSPEC package (v11.3) and included absorption due to the line-of-sight Galactic column density of N$_H = 1.91 \times 10^{20}$ cm^{-2} (Dickey & Lockman 1990). Hereafter, the quoted errors on the derived model parameters correspond to a 90% confidence level for one interesting parameter (i.e. $\Delta\chi^2 = 2.71$). Best-fit parameter values are given in the source-frame, unless otherwise specified.

As a first step, we fitted the *EPIC* spectra at energies above 3 keV using a simple power-law (PL) model in order to estimate the "hardness" of the X-ray continuum in 3C 234. This fit was very poor ($\chi^2_\nu \sim$3), with a ultra-flat pho-

Table 1. Best-fit spectral parameters of the *EPIC* spectrum. See Sect. 2.1 for details.

Model (1)	Γ (2)	N_H (3)	f_s (4)	$\Gamma_{\rm Soft}$ (5)	kT (6)	Flux (7)	Luminosity (8)	$EW_{K\alpha}$ (9)	χ^2(dof) (10)
(A)	$1.53^{+0.03}_{-0.04}$	$3.12^{+0.17}_{-0.17}$	0.05	$\equiv \Gamma$	$0.63^{+0.06}_{-0.07}$ $0.17^{+0.01}_{-0.01}$	0.83/13.27	0.06^*/2.61	139^{+42}_{-40}	282(254)
(B)	$1.71^{+0.05}_{-0.04}$	$3.69^{+0.19}_{-0.18}$	0.03	$1.09^{+0.13}_{-0.09}$	–	0.85/13.18	1.62/2.97	135^{+43}_{-41}	255(246)

The columns give the following information: (1) model (A: *baseline* model + two `mekal` components + unabsorbed PL, B: *baseline* model + soft X-ray Gaussian lines + unabsorbed PL); (2) photon index of the absorbed continuum power law; (3) the column density of the absorber (10^{23} cm^{-2}); (4) ratio between the normalization of the unabsorbed versus absorbed PL component at 1 keV; (5) photon index of the unabsorbed soft X-ray power law; (6) the temperature (keV) of the thermal plasma component (`mekal`); (7) the 0.5–2/2–10 keV observed flux (10^{-13} erg cm^{-2} s^{-1}); (8) the 0.5–2/2–10 keV luminosity (10^{44} erg s^{-1}); (9) EW of the Fe Kα line (eV); (10) χ^2 and number of degrees of freedom. * Luminosity of the thermal emission component in the 0.5–2.0 keV band.

ton index of $\Gamma \approx -0.4$ denoting the complexity of the X-ray emission in this source and, in particular, the presence of strong absorption. We then fitted the 3–10 keV spectrum with a model consisting of a combination of a PL (representing the primary continuum) absorbed by neutral matter at the redshift of the source and a narrow Gaussian line to account for the Fe Kα emission at 6.4 keV. This fit (hereafter indicated as *baseline* model) provides an excellent representation of the hard-band data, i.e. χ^2_ν(dof) = 1.04(162), revealing an X-ray primary continuum with slope $\Gamma \approx 1.5$ affected by a large amount of intrinsic absorption ($N_H \approx 3\times 10^{23}$ cm^{-2}).

The Fe Kα emission line shows a rest-frame energy of $E_{K\alpha}=6.38^{+0.03}_{-0.04}$ keV and an equivalent width $EW_{K\alpha} \approx 140\pm40$ eV. We obtained an upper limit on the line width of $\sigma_{K\alpha} < 120$ eV.

The extrapolation of this spectral model to the soft X-ray band showed the presence of several narrow emission features along with a smooth excess below $\sim$3 keV (e.g. Fig. 1). Such narrow features in the soft X-ray portion of the spectrum were initially modelled by the addition of a thermal plasma component (`mekal` in XSPEC) to the hard X-ray *baseline* model, under the hypothesis of an origin from starburst activity. This fit was completely unable to model the data at $E < 3$ keV with an associated $\chi^2_\nu \sim$6. We then added a second `mekal` component yielding a reasonable fit (χ^2(dof) =1.16(255)). However, some large data/model residuals remained around 0.8-0.9 keV (rest-frame). Furthermore, the temperature (and the 0.5-10 keV luminosity of $\approx 2 \times 10^{43}$ erg s^{-1} as well) measured for one of the thermal components, i.e. kT$\sim$8 keV, seems unlikely for a starburst region (Franceschini et al. 2003). It can be an artifact of the fit related to the difficulty of fitting the soft excess in the $\sim$1.5–3 keV band. Accordingly, we included an additional unabsorbed PL component fixing its photon index to that of the absorbed PL, as expected in case of scattered emission. The presence of the additional PL is required by the data at the $\gtrsim$ 99.8% confidence level. The temperatures of the two thermal components were $kT\approx$ 0.2 and $kT\approx$0.6 keV, respectively. The application of this model (e.g. Table 1, model A) to the data produces a pretty acceptable fit to the *EPIC* data with an associated χ^2_ν(dof) = 1.11(254) but leaves evident line-like positive residuals below 1 keV (see Fig. 2).

We then performed a phenomenological fit adding to the *baseline* model seven narrow Gaussian lines to account for the emission features observed in the $\sim$0.5–2 keV range. Each Gaussian line is required at a significance level of $P_F >$99.9% (except for the line at 2.44 keV with $P_F = 98.5\%$). However, due to the potential line blending with adjacent emission lines such a detection significance should be considered with care and, in some cases, it may represent only an upper limit. The photon index of the unabsorbed PL ($\Gamma_{\rm soft}$) was left free to vary since blends of unresolved emission lines appear as a pseudo-continuum when observed at the spectral resolution of *EPIC*. This PL component also accounts for a mixture of emissions caused by, i.e., the electron-scattered fraction of the primary continuum, thermal and/or photoionized plasma, the relativisic jet and Compton reflection off ionized matter (see Miniutti et al. 2007; Evans et al. 2006a; Turner et al. 1997), as observed in most of X-ray obscured AGNs. We yielded a very good description of the spectrum of 3C 234 (e.g. model B in Table 1), with an associated χ^2_ν(dof) = 1.04(246). The confidence contours for Γ versus N_H are plotted in Fig. 3. The ratio between the normalizations of the unabsorbed and absorbed PL is $f_s \approx 0.03$. In Table 2 the best-fit parameters are listed together with the likely identification for each of the soft X-ray lines.

Finally, the observed flux in the 2–10 keV band is $F_{2-10} \sim$1.3 $\times 10^{-12}$ erg cm^{-2} s^{-1}, which is consistent with the value measured with *ASCA* in 1994 (Sambruna et al. 1999).

3. Discussion

3.1. The Hard X–ray spectrum and the Fe Kα emission line

The *EPIC* observation presented here is the first good-quality X-ray spectrum of 3C 234 and, in general, it represents one of the best X-ray observation collected for a genuine QSO2 so far. Our analysis reveals the presence of a complex spectrum, largely dominated by strong obscuration. The X-ray continuum shows a slope of $\Gamma \sim 1.7$ and is absorbed by Compton-thin ($N_H \sim 3 \times 10^{23}$ cm^{-2}) neutral gas. Since the intrinsic 2–10 keV luminosity is $L_{2-10} \sim 3 \times 10^{44}$ erg s^{-1}, 3C 234 satisfies all the conditions to be considered a genuine Type 2 quasar.

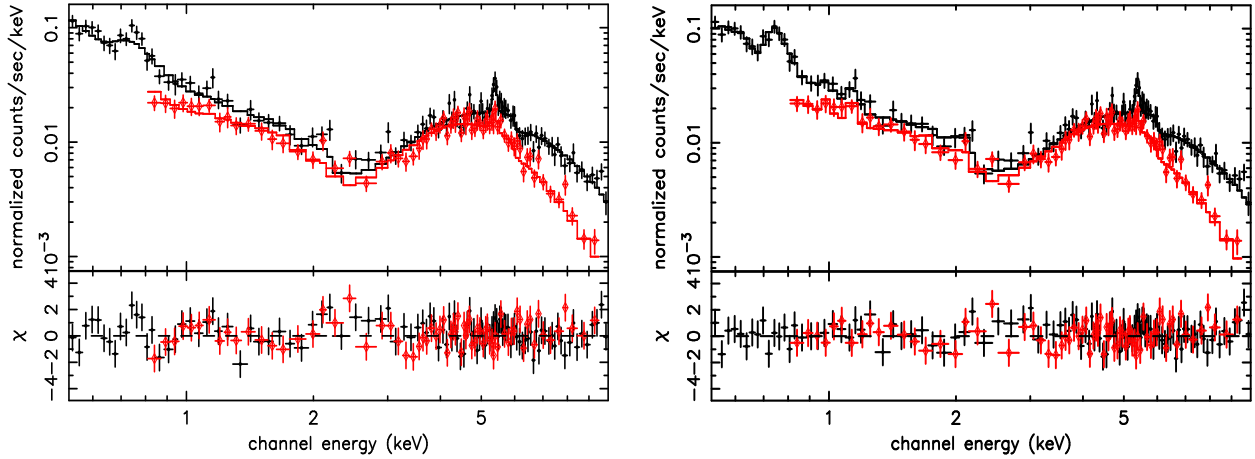**Fig. 2. (a)**–*Left: XMM–Newton PN* (top) and *MOS* (bottom) spectra of 3C 234 when the model A is applied. The lower panel shows the deviations of the observed data from the model in unit of standard deviation. **(b)**–*Right:* The same as in the left figure but for model B. See Table 1 for the best-fit parameters of each model.

Table 2. Best-fit spectral parameters for the emission lines detected in the soft X-ray band.

Energy (1)	Intensity (2)	P_F (3)	Identification (4)
$0.65^{+0.01}_{-0.01}$	$17.2^{+4.9}_{-2.7}$	>99.9	OVIII Lyα
$0.74^{+0.01}_{-0.02}$	$11.1^{+2.1}_{-1.9}$	>99.9	OVII RRC, Fe XVII 3s-2p
$0.89^{+0.01}_{-0.01}$	$12.3^{+1.2}_{-1.9}$	>99.9	OVIII RRC, NeIX Heα, Fe XVIII 3d-2p
$1.02^{+0.01}_{-0.02}$	$1.4^{+0.6}_{-0.9}$	>99.9	NeX Lyα, Fe XXI 3d-2p
$1.17^{\dagger}$	$1.8^{+0.6}_{-0.5}$	>99.9	FeXXIV L, NeX Lyβ, NeIX RRC
$1.34^{\dagger}$	$1.4^{+0.5}_{-0.5}$	>99.9	MgXI Heα
$2.44^{\dagger}$	$0.4^{+0.3}_{-0.1}$	98.5	SXV Heα

The columns give the following information: (1) Energy of the line (keV); (2) Intensity of the line (10^{-6} photons cm^{-2} s^{-1}); (3) Significance of the fit improvement after including the *Gaussian* line in the fitting model (based on F-test, see Sect. 2.1 for further details on this significance value); (4) Likely identification (e.g. Brinkman et al. 2002; Guainazzi & Bianchi 2007). † Indicates that the parameter has been fixed to the best-fit value deduced by the fit.

The value of the photon index of the continuum is consistent with the average value found for other lobe-dominated[1] FRII quasars, i.e. $\langle\Gamma\rangle \sim 1.6$–1.7 (Belsole et al. 2006; Piconcelli et al. 2005; Grandi et al. 2006). Harder photon indices of $\Gamma \sim 1.4$–1.5 are indeed usually observed in the core-dominated, more-aligned radio-loud AGNs, the so-called *Blazars*, whose featureless X-ray spectrum is dominated by relativistically-beamed inverse-Compton jet emission (e.g. Fossati et al. 1998; Donato et al. 2005). The *XMM–Newton* measurement implies that the jet contribu-
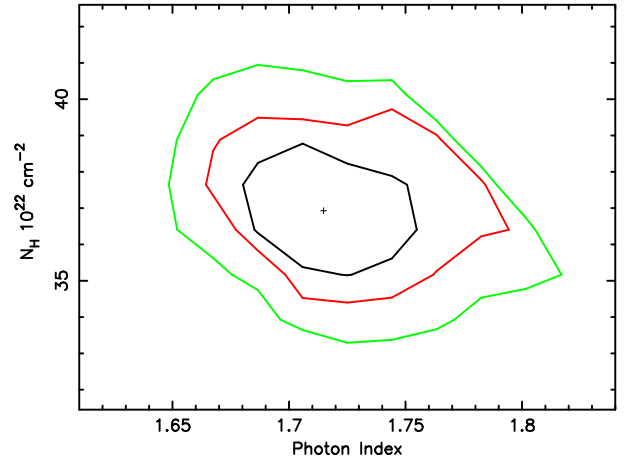
[1] Lobe-dominated radio-loud sources are those with a rest frame ratio (the so-called *core dominance* R$_c$) of radio core to lobe flux density of log R$_c$ <0 (Orr & Brown 1982). According to Sambruna et al. (1999) 3C 234 has a log R$_c$ = -1.34.

Fig. 3. Confidence contour plot showing the intrinsic rest–frame column density against the hard X-ray continuum photon index. The contours are at 68%, 90% and 99% confidence levels for two interesting parameters.

tion to the broad-band X-ray emission must be marginal as suggested by the detection of many soft X-ray emission lines as well as a prominent Fe Kα line at 6.4 keV in its spectrum. It is worth noting that this is the first time that such emission line has been detected at a statistically significant level in 3C 234. The best-fit rest-frame energy of the Fe Kα line is E$_{K\alpha}$=$6.38^{+0.03}_{-0.04}$ keV, corresponding to low ionization states, i.e. FeI–XVI (Kallman et al. 2004). The EW$\approx$140 eV of this line matches well with the value predicted by theoretical calculations (e.g. Awaki et al. 1991; Leahy & Creighton 1993; Ghisellini et al. 1994) for a Fe Kα line produced by transmission through an absorbing screen with a column of N$_H$ $\sim$3–4 $\times$ 10^{23} cm^{-2}, as that measured along the line of sight to the nucleus of 3C 234 by the *XMM–Newton* observation. This suggests that such Compton-thin absorber is the responsible for both obscuration and fluorescent narrow Fe Kα emission. However, the value of the EW is also consistent with reflection off distant Compton-thick matter (Guainazzi, Matt & Perola 2005). The cold reflector

could be then located at the far inner side of the molecular *torus* invoked in the AGN unified models (Antonucci 1993; see also Elitzur & Shlosman 2006) and seen along an unobscured line of sight. This scenario implies the simultaneous presence of two circumnuclear obscuring gases, one Compton-thick (the reflector) and one Compton-thin (the absorber), as recently discovered in some Seyfert 2 galaxies showing large X-ray spectral variations (Matt et al. 2003; Risaliti et al. 2005; Piconcelli et al. 2007b). If this is the case, the Compton-thin matter should cover only a small fraction of the sky (as seen by the X-ray primary source) in order not to produce too much iron Kα emission (Matt 2002). Furthermore the Fe Kα line should be accompanied by a Compton-reflection continuum emission peaking at $\sim$30 keV (Matt, Perola & Piro 1991; Krolik et al. 1994). Unfortunately, the limited *EPIC* bandpass does not allow to constrain meaningfully the strength of this spectral component in 3C 234, and, in turn, test the validity of this hypothesis. Future spectroscopy in the 10–60 keV range, say with *Simbol-X* (Ferrando et al. 2006), will be therefore crucial to disentangle between a transmission or a reflection origin for the Fe Kα line in this QSO2.

Young et al. (1998) inferred a dust extinction toward 3C 234 of $A_V = 60$ mag, which corresponds to an absorbing column density of $\approx 1.1 \times 10^{23}$ cm^{-2}, if the standard Galactic gas-to-dust ratio is assumed (i.e. $N_H/A_V = 1.79 \times 10^{21}$ cm^{-2} mag^{-1}, Predehl & Schmitt 1995), which is a factor of ~ 3.4 lower than observed. This mismatch has been observed in many X-ray sources as reported by Maiolino et al. (2001), that proposed the existence of dust grains larger than in the diffuse Galactic medium which do not redden efficiently the optical emission. Alternatively, Weingartner & Murray (2002) suggested that X-ray absorption and optical extinction occur in distinct regions, with the X-ray absorber located inside the dust sublimation radius.

3.1.1. The [Mg VIII] to 2–10 keV luminosity ratio

Imanishi (2006) reported the detection of a strong high-excitation emission line at 3.028 μm due to [Mg VIII], a hallmark of the presence of a powerful AGN in this source. We derive a [Mg VIII] to 2–10 keV luminosity ratio Mg^{7+}/X $=0.004$ assuming a [Mg VIII] luminosity $L_{Mg^{7+}} = 1.2 \times 10^{42}$ erg s^{-1}. Noteworthy, such a ratio is similar to that inferred for the archetypical Seyfert 2 galaxy Circinus, i.e. Mg^{7+}/X $=0.005$ using a $L_{Mg^{7+}} = 4.75 \times 10^{39}$ erg s^{-1}(Sturm et al. 2002) and a $L_{2-10} = 10^{42}$ erg s^{-1} (Matt et al. 1999), despite the fact that the $L_{Mg^{7+}}$ of the QSO2 is approximatively a factor of 250 larger than in Circinus. A value of Mg^{7+}/X $=0.004$ is also found for the heavily Compton-thick source NGC 1068 ($L_{Mg^{7+}} = 3.1 \times 10^{40}$ erg s^{-1}; Marco & Brooks 2003) if we adopt a $L_{2-10} = 7.7 \times 10^{42}$ erg s^{-1}, i.e. the value determined by Levenson et al. (2006) from the Fe Kα line luminosity (see also Panessa et al. 2006). The possibility of using $L_{Mg^{7+}}$ as a proxy of the intrinsic X-ray luminosity of an obscured active nucleus deserves further investigations, therefore a larger sample of AGN is needed to confirm this relationship on a more sound statistical ground. Unfortunately, an accurate measurement of the intensity [Mg VIII] emission line at 3.028 μm is available to date in literature only for a handful of sources.

3.2. The Soft X–ray emission

The emission lines detected for the first time at $\lesssim$ 2 keV in the *XMM–Newton* spectrum of 3C 234 (see Table 2) rule out the hypothesis that in this radiogalaxy the bulk of the soft X-ray emission arises from jet-related non-thermal emission, as suggested by Evans et al. (2006a) and Belsole et al. (2006) by the analysis of X-ray observations of narrow-line radio-loud AGNs. It is worth noting that a simple fit with an unabsorbed PL in the 0.5–2 keV band yields a very steep photon index ($\Gamma \sim 2.6$), which is in agreement with slopes of the soft X-ray PLs in absorbed FR II radio galaxies reported by Belsole et al. (2006).

Furthermore, as mentioned in Sect. 2.1, the 0.5–2 keV luminosity of $\approx 5.8 \times 10^{42}$ erg s^{-1} of the collisionally-heated plasma component (`mekal` in XSPEC) inferred by model A is too large to be associated with starburst regions, which typically show $10^{39} \lesssim L_{0.5-2} \lesssim$ a few times 10^{41} erg s^{-1} (e.g. Ptak et al. 1999; Franceschini et al. 2003). Using the relationship between far infrared (FIR) and soft X-ray luminosity reported by Ranalli et al. (2003) for a large sample of star-forming galaxies, we estimate a starburst luminosity of $L_{0.5-2}^{SB} \lesssim 3.3 \times 10^{41}$ erg s^{-1}, i.e. a contribution $\lesssim 4\%$ to the total soft X-ray observed luminosity in 3C 234 ($L_{0.5-2}^{Obs} = 8.2 \times 10^{42}$ erg s^{-1}), assuming a FIR luminosity of $L_{FIR} \lesssim 1.54 \times 10^{45}$ erg s^{-1}. According to Kennicutt (1998) the FIR luminosity of 3C 234 implies a star formation rate of SFR < 70 M$_\odot$ yr^{-1}, while a $L_{0.5-2} = 5.8 \times 10^{42}$ erg s^{-1} translates into a SFR ~ 1300 M$_\odot$ yr^{-1} (Ranalli et al. 2003), i.e. a very large value which is observed only in the most massive nuclear starbursts triggered by strong tidal interactions and mergers of galaxies. This finding is in agreement with the results of Imanishi (2006) that found in the 3–4 μ (*L*-band) spectrum of 3C 234 3.3 μm emission PAH features more than an order of magnitude weaker than those of typical starburst galaxies.

As the soft X-ray emission is not affected by absorption, the location of the emitting gas in this QSO2 must be far away from the obscuring gas intercepting the primary continuum.

The soft X-ray emission lines found by *XMM–Newton* can be associated (bearing in mind the EPIC resolution and the error bars of the energy values listed in Table 2) with hydrogen- and helium-like lines of the most abundant light metals, from oxygen to sulfur. This result is very similar to those reported from the *XMM–Newton* and *Chandra* observations of obscured radio-quiet Seyfert-like AGNs (e.g. Guainazzi & Bianchi 2007 and references therein), in which the soft X-ray emission is dominated by a wealth of emission lines and spatially coincident with the extended [OIII] emission (Iwasawa et al. 2003; Bianchi et al. 2006). High-resolution X-ray grating spectroscopy of this soft X-ray emission provides unambiguous evidence that most of it is produced in a photoionized outflowing gas (e.g. Kinkhabwala et al. 2002; Guainazzi & Bianchi 2007). On the other hand, the exact physical mechanism generating the emission-line spectra is still debated. Both AGN-photoionization and "local" photoionization due to gas heated by high-speed shocks driven by nuclear outflows (i.e. the radio jet) in the interstellar medium (Fu & Stockton 2006; Evans et al. 2006b) are viable mechanisms.

This scenario could likely hold also in 3C 234 even if this source is a radio-loud QSO2. In particular, the detection

of two prominent lines at 0.74 and 0.88 keV bolsters this hypothesis since they may be associated with narrow OVII and OVIII Radiative Recombination Continuum (RRC), respectively, which are hallmarks of recombination in a low-temperature photoionized plasma (Liedahl 1999). However, better quality high-resolution spectral data are necessary before a firm conclusion can be drawn on the exact origin of these emission lines. Due to the weakness of 3C 234 in the soft X-ray band ($F_{0.5-2} \approx 8 \times 10^{-14}$ erg cm^{-2} s^{-1}) no meaningful RGS data were collected during the present *XMM–Newton* observation. This does not allow to estimate the possible contribution arising from collisionally-ionized plasma.

The discovery of a rich emission-line soft X-ray spectrum in 3C 234 is noteworthy since this is the first time it has been found in a Type 2 and, even more remarkable, radio-loud QSO. In fact, only very recently Sambruna et al. (2007) and Grandi et al. (2007) reported the first clearcut example of a radio-loud AGN with a soft X-ray spectrum dominated by emission lines on the basis of the *XMM–Newton* observation of the heavily absorbed FRII radio galaxy 3C 445 (e.g. also Young et al. 2002). These findings suggest that inner circumnuclear regions in radio-loud (in particular those with high excitation optical emission lines, which usually show a FRII radio morphology, e.g. Grandi & Palumbo 2007; Ballantyne 2007) and radio-quiet AGNs could have similar geometrical and physical properties.

Finally, according to model B the unabsorbed PL has a photon index of $\Gamma_{\rm Soft} = 1.09^{+0.13}_{-0.09}$. The 0.5–2 keV luminosity of this spectral component is $L_{0.5-2} \approx 4 \times 10^{42}$ erg s^{-1}, which represents about 2–3% of the intrinsic luminosity of 3C 234 in the soft X-ray band ($\approx 1.6 \times 10^{44}$ erg s^{-1}). This emission could be due to a blend of nuclear scattered emission arising from the line-emitting warm photoionized plasma (and/or the electron mirror located interior to the NLR proposed by T95 on the basis of spectropolarimetric data) and unresolved X-ray emitting knots of the kpc-scale jet (which usually show flat X-ray slope, $\Gamma \approx 1.0$–1.3; e.g. Sambruna et al. 2004), plus a possible, marginal (i.e. < 8%, assuming a starburst luminosity of $L^{SB}_{0.5-2} < 3.3 \times 10^{41}$ erg s^{-1} estimated from the FIR luminosity of 3C 234; e.g. Ranalli et al. 2003) contribution from X-ray binaries.

4. Summary

In this paper, we present the analysis of the *XMM–Newton* observation of 3C 234 collected in 2006. These data provide the most detailed description to date of the X-ray spectral properties of this FRII radio galaxy, which has been long known for hosting a hidden quasar at its center (Antonucci & Barvainis 1990).

The quality of the data allows to shed light on many controversial issues about the characteristics of the X–ray emission in 3C 234, i.e. the exact shape of the continuum, the iron K fluorescent emission and the nature of the soft X-ray spectral component, left unsettled by the low signal-to-noise ratio 1994 *ASCA* observation. We measure a $L_{2-10} \approx 3 \times 10^{44}$ erg s^{-1}, whereby 3C 234 falls well within the quasar X-ray luminosity range (Fabian 2003). At face value, the 0.5–10 keV spectrum of this radio-loud QSO2 is typical of a nearby Compton-thin Seyfert 2 galaxy. It is dominated by heavy obscuration ($N_{\rm H} \sim 3.7 \times 10^{23}$ cm^{-2}), with a strong,

narrow Fe Kα emission line at 6.4 keV and many emission lines from highly ionized metals in the soft X-ray band. Such a line-rich spectrum and the steepness of the hard X-ray continuum, $\Gamma \approx 1.7$, reveal that the non-thermal emission arising from the relativistic jet provides a marginal contribution to the X-ray emission. The strength of the Fe Kα line is fairly consistent with that expected in transmission from the observed obscuring screen with $N_{\rm H} \sim 4 \times 10^{23}$ cm^{-2}. However, a line origin from reflection occuring at the AGN-illuminated, far inner surface of the Compton-thick *torus* cannot be rule out. This in turn would imply the presence of two absorbing regions coexisting in this QSO2.

The detection of lines at 0.74 and 0.87 keV (i.e. the energy of the narrow OVII and OVIII RRC, respectively) strongly indicates that most of the soft X-ray emission originates from a photoionized plasma. The presence of this warm gas is particularly important since it suggests that the circumnuclear environment in radio-loud and radio-quiet AGNs share the same geometrical and physical properties. This remarkable finding leads support to recent *XMM–Newton* results (e.g. Grandi et al. 2007; Sambruna et al. 2007), which reported a similar scenario for 3C 445, another X-ray luminous, obscured FRII radio galaxy.

References

Akiyama, M., Ueda, Y., Ohta, K., 2002, ApJ, 567, 42
Akylas, A., Georgantopoulos, I., Georgakakis, A., Kitsionas, S., Hatziminaoglou, E., 2006, A&A, 459, 693
Antonucci, R., 1993, ARA&A, 31, 473
Antonucci, R., 1984, ApJ, 278, 499
Antonucci, R., 1982, Nature, 299, 605
Antonucci, R., Barvainis, R., 1990, ApJ, 363, L17
Avni, Y., 1976, ApJ, 210, 642
Awaki, H., Murakami, H., Ogawa, Y., Leighly, K. M., 2006, ApJ, 645, 928
Ballantyne, D. R., 2007, Modern Physics Letters A, in press, (astro-ph/0707.3142)
Belsole, E., Worrall, D. M., Hardcastle, M. J., 2006, MNRAS, 366, 339
Bianchi, S., Guainazzi, M., Chiaberge, M., 2006, A&A, 448, 499
Brandt, W. N., Hasinger, G., 2005, ARA&A, 43, 827
Brandt, W. N., Fabian, A. C., Takahashi, K., Fujimoto, R., Yamashita, A., Inoue, H., Ogasaka, Y., 1997, MNRAS, 290, 617
Brinkman, A. C., et al., 2002, A&A, 396, 761
Cohen, M. H., Ogle, P. M.. Tran. H. D., Goodrich, R. W., Miller, J. S., 1999, AJ, 118, 1963
Dickey, J. M., Lockman, F. J. 1990, ARA&A. 28, 215
Della Ceca, R., et al., 2003, A&A, 406, 555
Derry, P. M., O'Brien, P. T., Reeves, J. N., Ward, M. J., Imanishi, M., Ueno, S.
Donato, D., Sambruna, R. M., Gliozzi, M., 2005, A&A, 433, 1163
Eckart, M. E., Stern, D., Helfand, D. J., Harrison, F. A., Mao, P. H., Yost, S. A., 2006, ApJS, 165, 19
Elitzur, M., Shlosman, I., 2006, ApJ, 648, L101
Evans, D. A., Worrall, D. M., Hardcastle, M. J., Kraft, R. P., Birkinshaw, M., 2006a, ApJ, 642, 96
Evans, D. A., Lee, J. C., Kamenetska, M., Gallagher, S. C., Kraft, R. P., Hardcastle, M. J., Weaver, K. A., 2006b, ApJ,653,1121
Fabian, A. C. 2003, Carnegie Observatories Astrophysics Ser., vol. I, ed. L. Ho. (Cambridge University Press) (astro-ph/0304122)

Ferrando, P., et al., 2006, Proc. of the SPIE, 6266, 62660F
Fiore, F., et al., 2003, A&A, 409, 79
Franceschini, A., et al., 2003, MNRAS, 343, 1181
Franceschini, A., Bassani, L., Cappi, M., Granato, G. L., Malaguti,G., Palazzi, E., Persic, M. 2000, A&A, 353, 910
Fossati, G., Maraschi, L., Celotti, A., Comastri, A., Ghisellini, G., 1998, MNRAS, 299, 433
Fu, H., Stockton, A., 2006, ApJ, 650, 80
Gandhi, P., Fabian, A. C., Crawford, C. S., 2006, MNRAS, 369, 1566
Georgantopoulos, I., Georgakakis, A., Akylas, A., 2007, A&A, 466, 823
Gilli, R., Comastri, A., Hasinger, G., 2007, A&A, 463, 79
Ghisellini, G., Haardt, F., Matt, G. 1994, MNRAS, 267, 743
Grandi, P., Palumbo, G. G. C., 2007, ApJ, 659, 235
Grandi, P., Guainazzi, M., Cappi, M., Ponti, G., 2007, MNRAS, 381, L21
Grandi, P., Malaguti, G., Fiocchi, M., 2006, ApJ, 642, 113
Grandi, S.A., Osterbrock, D. E., 1978, ApJ, 220, 783
Guainazzi, M., & Bianchi, S., 2007, MNRAS, 374, 1290
Guainazzi, M., Matt, G., Perola, G. C., 2005, A&A, 444,119
Halpern, J. P., Turner, T. J., George, I. M., 1999, MNRAS, 307, L47
Houck, J.R., et al., 2005, ApJ, 622, L105
Imanishi, M., 2006, AJ, 131, 2406
Iwasawa, K., Crawford, C. S., Fabian, A. C., Wilman, R. J., 2005, MNRAS, 362, L20
Iwasawa, K., Wilson, A. S., Fabian, A. C., Young, A. J., 2003, MNRAS, 345, 369
Jansen, F., et al., 2001, A&A, 365, L1
Kallman, T. R., Palmeri, P., Bautista, M. A., Mendoza, C., Krolik, J. H., 2004, ApJS, 155, 675
Kennicutt, R. C., 1998, ARA&A, 36, 189
Kinkhabwala, A., Sako, M., Behar, E., et al., 2002, ApJ, 575, 732
Kirsch, M., 2006, "EPIC status of calibration and data analysis", XMM-SOC-CAL-TN-0018, Issue 2.5
Kishimoto, M., Antonucci, R., Cimatti, A., Hurt, T., Dey, A., van Breugel, W., Spinrad, H., 2001, ApJ, 547, 667
Krolik, J. H., Madau, P., Zycki, P. T., 1994, ApJ, 420, L57
La Franca, F., et al., 2005, ApJ, 635, 864
Lacy, M., et al., 2007, AJ, 133, 186
Leahy, D. A., Creighton, J., 1993, MNRAS, 263, 314
Levenson, N. A., Heckman, T. M., Krolik, J. H., Weaver, K. A., Zycki, P. T., 2006, ApJ, 648, 111
Liedahl, D. A. 1999, in X-Ray Spectrocopy in Astrophysics, ed. J. van Paradijs & J. A. M. Bleeker (Berlin: Springer), 189
Maiolino, R., et al., 2006, A&A, 445, 457
Maiolino, R., et al., 2001, A&A, 365, 28
Mainieri, V., et al., 2002, A&A, 393, 425
Marco, O., Brooks, K. J., 2003, A&A, 398, 101
Martinez-Sansigre, A., 2005, Nature, 436, 666
Matt, G., 2002, MNRAS, 337, 147
Matt, G., Guainazzi, M., Maiolino, R., 2003, MNRAS, 342, 422
Matt, G., Perola, G. C., Piro, L., 1991, A&A, 247, 25
Matt et al., 1999, A&A, 341, L39
Miniutti, G., Ponti, G., Dadina, M., Cappi, M., Malaguti, G., 2007, MNRAS, 375, 227
Norman, C., et al., 2002, ApJ, 571, 218
Orr, M. J. L., Browne, I. W. A., 1982, MNRAS, 200, 1067
Panessa, F., et al., 2006, A&A, 455, 173
Piconcelli, E., Fiore, F., Nicastro, F., Mathur, S., Brusa, M., Comastri, A., Puccetti, S., 2007a, A&A, 473, 85
Piconcelli, E., Bianchi, S., Guainazzi, M., Fiore, F., Chiaberge, M., 2007b, A&A,466, 855
Piconcelli, E., Guainazzi, M., Cappi, M., Jimenez-Bailon, E., Schartel, N., 2005, A&A, 432, 835
Piconcelli, E., Jimenez-Bailon, E., Guainazzi, M., et al., 2004, MNRAS, 351, 161
Piconcelli, E., Cappi, M., Bassani, L., Di Cocco, G., Dadina, M., 2003, A&A, 412, 689
Predehl, P.; Schmitt, J. H. M. M., 1995, A&A, 293, 889
Ptak, A., Zakamska, N. L., Strauss, M. A., Krolik, J. H., Heckman, T. M., Schneider, D. P., Brinkmann, J., 2006, ApJ, 637, 147
Ptak, A., Serlemitsos, P., Yaqoob, T., Mushotzky, R., 1999, ApJS, 120, 179
Ranalli, P., Comastri, A., Setti, G., 2003, A&A, 399, 39
Riley, J. M., Pooley, G. G., 1975, MmRAS, 80, 105
Risaliti, G., Elvis, M., Fabbiano, G., Baldi, A., Zezas, A., 2005 ApJ, 623, L93
Tran, H. D., Cohen, M.H., Goodrich, R. W., 1995, AJ, 110, 2597

Turner, T. J., George, I. M., Nandra, K., Mushotzky, R. F. 1997, ApJS, 113, 23 Sambruna, R. M., Reeves, J. N., Braito, V., 2007, ApJ, 665, 1030
Sambruna, R. M., Eracleous, M., Mushotzky, R. F., 1999, ApJ, 526, 60
Sambruna, R. M., Reeves, J. N., Braito, V., 2007, ApJ, 665, 1030
Sambruna, R., et al., 2004, ApJ, 608, 698
Severgnini, P., et al., 2006, A&A, 451, 859
Spergel, D.N., et al., 2007, ApJS, 170, 377
Steffen, A. T., Barger, A. J., Cowie, L. L., Mushotzky, R. F., Yang, Y., 2003, ApJ, 596, L23
Stern, D., et al. 2002, 568, 71
Sturm, E., et al., 2002, A&A, 393, 821
Tran, H. D., Cohen, M. H., Goodrich, R. W., 1995, AJ, 110, 2597 (T95)
Ueda, Y., et al., 2003, ApJ, 598, 886
Urry, C. M., Padovani, P., 1995, PASP, 107, 803
Vignali, C., Alexander, D. M., Comastri, A., 2006, MNRAS, 373, 321
Wang, X. C., et al., 2007, ApJ, 657, 95
Weingartner, J. C., Murray, N., 2002, ApJ, 580, 88
Young, S., Hough, J. H., Axon, D. J., Fabian, A. C., Ward, M. J., 1998, MNRAS, 294, 478
Young, A. J., Wilson, A. S., Terashima, Y., Arnaud, K. A., Smith, D. A., 2002, ApJ, 564, 176